Synthesis, Characterization, Self-assembly and Physical Properties of 11-Methyl-benzo[d]pyreno[4,5-b]furan

Jinchong Xiao,[†‡] Bo Yang,[†‡] Jen It Wong,[ǂ] Yi Liu,[†] Fengxia Wei,[†] Ke Jie Tan,[†] Xue Teng,[§] Yuechao Wu,[†] Ling Huang, [§]Christian Kloc,[†] Freddy Boey,[†] Jan Ma,[†] Hua Zhang,[†] Huiying Yang,[ǂ] Qichun Zhang[†]*

[†]School of Materials Science and Engineering, Nanyang Technological University, 50 Nanyang Avenue, Singapore 639798 (Singapore); [‡]College of Chemistry and Environment Science, Hebei University, Baoding, P. R. China; [ǂ]Pillar of Engineering Product Development, Singapore University of Technology and Design, 287 Ghim Moh Road, Singapore 279623 (Singapore). [§]School of Chemical Biological and Engineering, Nanyang Technological University, 50 Nanyang Avenue, Singapore 639798(Singapore)

qczhang@ntu.edu.sg

ABSTRACT

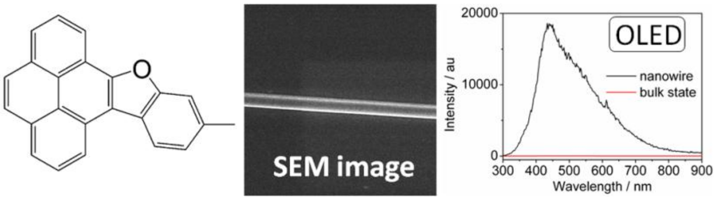

Synthesis, structure and physical properties of a novel 11-methyl-benzo[*d*]pyreno[4,5-*b*]furan (**BPF**) and its self-assembly in water have been reported. The performance of nanowire-based films in organic light-emitting diodes is much better than that of the thin film deposited by directly drop-coating **BPF** molecules in THF solution. SEM study indicates that the well-organized structure (nanowires) is an important factor in enhancing the performance of OLED devices.

Organic conjugated small molecules have received continuous attention because of their wide applications in organic electronic devices such as light-emitting diodes (OLED), field-effect transistors, and solar cells.[1,2] In particular, OLEDs are being considered as future lighting tools to replace our current lighting system because of their high energy efficiency and longer life time.[3] Moreover, the flexibility of organic materials, which can allow us to make all kinds of shapes (twisting, bending, and stretching) and can adapt themselves to any rough surfaces, makes them more promising in practical applications.[4] In addition, one-dimensional self-assembly of these conjugated molecules has attracted increasing interest in organic electronics.[5] The low stiffness and high elasticity of the organic-wire-based films endow the devices with the capability for large reversible deformation. Such devices are highly desirable for a broad range of applications because of their conformability, low stowed volume, and compatibility with low-cost impact resistance.

Pyrene and its derivatives have attracted considerable interest because they have high thermal stability, photoluminescence (PL) efficiency together with enhanced hole injection ability.[6] More efforts have been made to synthesize new pyrene-based derivatives and to control their morphologies through the assistance of various weak interactions such as H-bonding, π-π stacking, electrostatic interaction, and solvophobic effect.[7] On the other hand, benzo[*b*]furan and its derivatives not only have interesting optical properties such as fluorescence and radioluminescence, but also are the core structural elements in natural and synthetic organic compounds.[8] The integration of pyrene species and benzo[*b*]furan units into one molecule could generate a novel emitter with a new phenomenon for OLEDs. In this paper, we report the synthesis of a novel molecule 11-methyl-benzo[*d*]pyreno[4,5-*b*]furan (**BPF**, Scheme 1), self-assembly of **BPF** into nanowires, and their performance (both nanowires and molecules) in OLEDs.

The synthetic route of compound 11-methylbenzo[*d*]pyreno[4,5-*b*]furan (**BPF**) is described in Scheme 2. **BPF** was obtained as a light yellow solid in 36 % yield by condensation reaction between pyrene-4,5-dione[9] and 3-methylphenol in the presence of trifluoromethanesulfonic acid (Scheme 2). The novel compound **BPF** was fully characterized by FT-IR, ^{1}H NMR, ^{13}C NMR, MALDI-TOF, and HR mass spectroscopes (Figure S1-S5 of Supporting Information). **BPF** is soluble in common organic solvents such as toluene, CH_2Cl_2, $CHCl_3$, THF, acetonitrile, methanol, and *N*,*N*-dimethylformamide. The self-assembled nanowires of **BPF** were obtained through reprecipitation by adding a THF solution of **BPF** into water containing poly(ethylene glycol)-block-poly (propylene glycol)-block-poly(ethylene glycol) (P123) surfactant. The SEM and TEM studies of as-prepared nanowires have been performed and will be discussed in the following part.

Needle-like single crystals of **BPF** were obtained through physical transport sublimation. The crystal structure of **BPF**, displayed in Figure 1a, clearly shows that pyrene unit and benzo[b]furan part are in one plane, which is different from a previously reported twisted system from our group.[2a,2b,10] Figure 1b presented a packing diagram for compound **BPF**. The interlayer face-to-face stacking was observed and the interplanar distance of **BPF** molecules was 3.40 Å, which indicates that there exists strong π-stacking in neighboring molecules.

The self-assembled **BPF** nanowires were characterized by SEM and TEM. As shown in Figure 2a, **BPF** readily forms nanowires by addition of a THF solution of **BPF** into an aqueous solution containing P123 block polymer as the surfactant. The as-prepared wires have the diameters in the range of 150-300 nm and lengths of 3-20 μm. The TEM study furthermore confirms the nanostructures' morphology obtained from SEM. The selected area electron diffraction (SAED) pattern (Figure 2d) indicates that the as-prepared nanowires are crystalline. The crystallinity was furthermore confirmed by X-ray diffraction (XRD). As shown in Figure 2b, the XRD results was indexed in space group C2/c with “standard” lattice constants (a = 49.52 Å, b = 4.861 Å, c = 40.62 Å and β = 116.289 °). Based on the XRD patterns of **BPF** nanowires and simulation, one can know that the obtained nanowires are single crystals and the preferential orientation is the $(40\bar{4})$ lattice plane.

The UV-vis and fluorescence spectra for **BPF** molecules in THF solution and nanowires in aqueous solution are shown in Figure 3. **BPF** in THF solution displays the absorption peaks at 340, 356, and 381 nm and the emission maxima at 380, 402, 425 and 460 nm (excited at 356 nm, Figure 3). Interestingly, the UV-vis absorption of nanowires becomes broad and dramatically red-shifted compared to that of **BPF** in THF solution, which is believed to come from J-type aggregation of **BPF** molecules.[11] No surprisingly, the emission peaks are also red-shifted to 430, 458, 505, 542 nm, which further confirmed the formation of J-type aggregation. It should be noted that similar absorption bands and emission spectra were also observed in thin film (Figure S6, Supporting Information). The quantum yield of **BPF** molecules in THF and nanowires in aqueous solution were measured as Φ_f = 0.27 and 0.12, respectively, using 9,10-diphenylanthracene as the standard (Φ_f = 0.95 in ethanol[7a]) at room temperature (excited at 356 nm). Note that the quantum yield of **BPF** nanowires was ~2 times less than that of **BPF** in THF solution.

FT-IR was performed to test the absence of P123 in nanowires (Figure S7, Supporting Information). Figure 4 shows EL spectra from the heterojunction LED of bulk and nanowires under a forward bias of 30.5 V. The structure of electroluminescent device is ITO/**BPF** bulk or nanowires/*n*-SiC/Ti/Au. The spectra were measured by connecting the cathode and anode of a constant voltage source to the ITO and Ti/Au metal contacts of the heterojunction, respectively. Light was collected from the surface of the ITO glass by an optical fiber to a PMT detector. It is found that the emission spectrum of nanowire-based LEDs can be fitted by four Gaussian curves with peak wavelengths at ~438, ~524, ~607 and ~668 nm (Figure S8a, Supporting Information), while the EL spectrum from bulk **BPF** shows a very broad emission which centered at a wavelength of ~583 nm (Figure S8b, Supporting Information). It was noted that no emission was observed from the heterojunction LED under a reverse bias, which suggested that a heterojunction is formed between the p-organic nanostructure and *n*-SiC. These EL spectra also show that the emission intensities in nanowires and bulk materials are highly different. The emission intensity of nanowires is approximately 50 times larger than that of bulk materials. The SEM study (Figure S9 of Supporting Information) on two films indicates that nanowire-based film has a better morphology than that of the thin film deposited by directly drop-coating **BPF** molecules in THF solution. This result demonstrated that morphology control is very important in the enhancement of the performance of heterojunction light emitting diode (LED) devices.

In conclusion, a new compound **BPF** and its self-assembled nanowires were successfully prepared. The single crystal structure shows that **BPF** is a conjugated plane molecule. Further investigation of the performance of the bulk state and nanowires in OLED devices suggested that the nanowire-based film does show better performance than that deposited through drop-coating

BPF molecules. This result could be helpful in optimizing the devices' performance through control of their shapes.

ACKNOWLEDGEMENT

Q.Z. acknowledges financial support from Nanyang Technological University (start-up grant) and the AcRF Tier 1 (RG 18/09) from MOE.

SUPPORTING INFORMATION AVAILABLE

Synthetic and experimental procedures, spectral characterization data for **BPF**, and X-ray crystallographic data of **BPF** (CIF). This material is available free of charge via the Internet at http://pubs.acs.org.

Reference

(1) (a) Pron, A.; Gawrys, P.; Zagorska, M.; Djurado, D.; Demadrille, R. *Chem. Soc. Rev.* **2010**, *39*, 2577. (b) Anthony, J. E. *Chem. Rev.* **2006**, *106*, 5028. (c) Hoeben, F. J. M.; Jonkheijm, P.; Meijer, E. W.; Schenning, A. P. H. J. *Chem. Rev.* **2005**, *105*, 1491.

(2) (a) Xiao, J.; Divayana, Y.; Zhang, Q.; Doung, H. M.; Zhang, H.; Boey, F.; Sun, X.; Wudl, F. *J. Mater. Chem.* **2010**, *20*, 8167. (b) Zhang, Q.; Divayana, Y.; Xiao, J.; Wang, Z.; Tiekink, E. R. T.; Doung, H. M.; Zhang, H.; Boey, F.; Sun, X.; Wudl, F. *Chem. Eur. J.* **2010**, *16*, 7422. (c) Yang, Y.; Wudl, F. *Adv. Mater.* **2009**, *21*, 1401. (d) Blouin, N.; Michaud, A.; Gendron, D.; Wakim, S.; Blair, E.; Neagu-Plesu, R.; Belletête, M.; Durocher, G.; Tao, Y.; Leclerc, M. *J. Am. Chem. Soc.* **2008**, *130*, 732. (e) Schmidt-Mende, L.; Fechtenkötter, Müllen, K.; Moons, E.; Friend, R. H.; MacKenzie, J. D. *Science* **2001**, *293*, 1119.

(3) (a) Bartelmess, J.; Ballesteros, B.; Torre, G. D. A.; Kiessling, D.; Campidelli, S.; Prato, M.; Torres, T.; Guldi, D. M. *J. Am. Chem. Soc.* **2010**, *132*, 16202. (b) Zhou, Y.; Kim, J. W.; Kim, J. M.; Son, W. J.; Han, S. J.; Kim, H. N.; Han, S.; Kim, Y.; Lee, C.; Kim, S. J.; Kim, D. H.; Kim, J. J.; Yoon, J. *Org. Lett.* **2010**, *12*, 1272. (c) Diring, S.; Camerel, F.; Donnio, B.; Dintzer, T.; Toffanin, S.; Capelli, R.; Muccini, M.; Ziessel, R. *J. Am. Chem. Soc.* **2009**, *131*, 18177. (d) Figuera-Duarte, T. M.; Simon, S. C.; Wagner, M.; Druzhinin, S. I.; Zachariasse, K. A.; Müllen, K. *Angew. Chem. Int. Ed.* **2008**, *47*, 10175.

(4) (a) Rogers, J. A.; Someya, T.; Huang Y. *Science*, **2010**, *327*, 1603. (b) Rogers, J. A.; Huang Y. *Proc. Natl. Acad. Sci. USA*, **2009**, *106*, 10875. (c) Gelinck G. H.; Huitema, H. E. A.; Veenendaal, E. V.; Cantatore, E.; Schrijnemakers, L.; Van Der Putten, J. B. P. H.; Geuns, T. C. T.; Beenhakkers, M.; Giesbers, J. B.; Huisman, B.-H.; Meijer, E. J.; Benito, E. M.; Touwslarger, F. J.; Marsman, A. W.; Van Rens, B. J. E.; De Leeuw, D. M. *Nat. Mater*. **2004**, *3*, 106.

(5) (a) Xiao, J.; Kusuma, D. Y. ; Wu, Y.; Boey, F.; Zhang, H.; Lee, P. S.; Zhang, Q. *Chem Asian J.* **2011**, *6*, 801. (b) Xiao, J.; Yin, Z.; Li, H.; Zhang, Q.; Boey, F.; Zhang, H.; Zhang, Q. *J. Am. Chem. Soc.* **2010**, *132*, 6926. (c) Zhao, Y. S.; Wu, J.; Huang, J. *J. Am. Chem. Soc.* **2009**, *131*, 3158. (d) Zang, L.; Che, Y.; Moore, J. S. *Acc. Chem. Res.* **2008**, *41*, 1596. (e) Briseno, A. L.; Mannsfeld, S. C. B.; Lu, X.; Xiong, Y.; Jenekhe, S. A.; Bao, Z.; Xia, Y. *Nano Lett.* **2007**, *7*, 668. (f) Liu, H.; Li, Y.; Xiao, S.; Gan, H.; Jiu, T.; Li, H.; Jiang, L.; Zhu, D.; Yu, D.; Xiang, B.; Chen, Y. *J. Am. Chem. Soc.* **2003**, *125*, 10794. (g) Liu, H.; Li, Y.; Jiang, L.; Luo, H.; Xiao, S.; Fang, H.; Li, H.; Zhu, D.; Yu, D.; Xu, J.; Xiang, B. *J. Am. Chem. Soc.* **2002**, *124*, 13370. (h) Xu, J.; Wen, L.; Zhou, W.; Lv, J.; Guo, Y.; Zhu, M.; Liu, H.; Li, Y.; Jiang, L. *J. Phys. Chem. C* **2009**, *113*, 5924. (i) Xu, J.; Liu, X.; Lv, J.; Zhu, M.; Huang, C.; Zhou, W.; Yin, X.; Liu, H.; Li, Y.; Ye, J. *Langmuir* **2008**, *24*, 4231.

(6) (a) Zhao, Z.; Chen, S.; Lam, J. W. Y.; Lu, P.; Zhong, Y.; Wong, K. S.; Kwok, H. S.; Tang, B. Z. *Chem. Commun*. **2010**, *46*, 2221. (b) Oh, H. Y.; Lee, C.; Lee, S. *Org. Electronics* **2009**, *10*, 163. (c) Tang, C.; Liu, F.; Xia, Y.-J.; Lin, J.; Xie, L. H.; Zhong, G. Y. ; Fan, Q. L. ; Huang, W.

Org. Electronics **2006**, *7*, 155. (d) Tang, C.; Liu, F.; Xie, L. H.; Wei, A.; Li, S. B.; Fan, Q. L.; Huang, W. *J. Mater. Chem.* **2006**, *16*, 4074.

(7) (a) Xiao, J.; Yang, H.; Yin, Z.; Guo, J.; Boey, F.; Zhang, H.; Zhang, Q. *J. Mater. Chem.* **2011**, *21*, 1423. (b) Yagai, S.; Aonuma, H.; Kikkawa, Y.; Kubota, S.; Karatsu, T.; Kitamura, A.; Mahesh, S.; Ajayaghosh, A. *Chem. Eur. J.* **2010**, *16*, 8652. (c) Häner, R.; Samain, F.; Malinovskii, V. L. *Chem. Eur. J.* **2009**, *15*, 5701. (d) Diring, S.; Camerel, F.; Donnio, B.; Dintzer, T.; Toffanin, S.; Capelli, R.; Muccini, M.; Ziessel, R. *J. Am. Chem. Soc.* **2009**, *131*, 18177. (e) Xiao, J. C.; Xu, J. L.; Cui, S.; Liu, H. B.; Wang, S.; Li, Y. L. *Org. Lett.* **2008**, *10*, 645. (f) Kamikawa, Y.; Kato, T. *Org. Lett.* **2006**, *8*, 2463. (g) Xu, Q.; Duong, H. M.; Wudl, F.; Yang, Y. *Appl. Phys. Lett.* **2004**, *85*, 3357.

(8) (a) Pickett, S. D.; Green, D. V. S.; Hunt, D. L.; Pardoe, D. A.; Hughes, I. *ACS Med. Chem. Lett.* **2011**, *2*, 28. (b) Cramp, S.; Dyke, H. J.; Higgs, C.; Clark, D. E.; Gill, M.; Savy, P.; Jennings, N.; Price, S.; Lockey, P. M.; Norman, D.; Porres, S.; Wilson, F.; Jones, A.; Ramsden, N.; Mangano, R.; Leggate, D.; Andersson, M.; Hale, R. *Bioorg. Med. Chem. Lett.* **2010**, *20*, 2516. (c) Thalji, R. K.; Aiyar, N.; Davenport, E. A.; Erhardt, J. A.; Kallal, L. A.; Morrow, D. M.; Senadhi, S.; Burns-Kurtis, C. L.; Marino Jr, J. P. *Bioorg. Med. Chem. Lett.* **2010**, *20*, 4104. (d) Tsuji, H.; Mitsui, C.; Sato, Y.; Nakamura, E. *Adv. Mater.* **2009**, *21*, 3776. (e) Kraus, G. A.; Gupta, V. *Tetrahedron Lett.* **2009**, *50,* 7180. (f) Shukla, R.; Wadumethrige, S. H.; Lindeman, S. V.; Rathore, R. *Org. Lett.* **2008**, *10*, 3587. (g) Liang, Z. Q.; Ma, S. M.; Yu, J. H.; Xu, R. R. *Tetrahedron* **2007**, *63*, 12877.

(9) Hu, J.; Zhang, D.; Harris, F. W. *J. Org. Chem.* **2005**, *70*, 707.

(10) Duong, H. M.; Bendikov, M.; Steiger, D.; Zhang, Q.; Sonmez, G.; Yamada, J.; Wudl, F. *Org. Lett.* **2003**, *5*, 4433.

(11) (a) MaRae, E.G.; Kasha, M. *Physical Processes in Radiation Biology*; Augenstein, Rosenberg and Mason, Eds.; Academic Press: New York, 1964. (b) Lee, T. W.; Park, O. O. *Adv. Mater*. **2000**,12,801.

List of schemes

Scheme 1. Chemical Structure of Compound **BPF**.

Scheme 2. Synthetic Route of Compound **BPF** (**1**).

List of Figures

Figure 1. (a) Single crystal and (b) molecular packing of **BPF**. Carbon and oxygen atoms are colored in gray and red, respectively.

Figure 2. (a) FESEM image of self-assembled **BPF** nanowires. The inset shows a magnified typical nanowire. (b) XRD patterns of **BPF** nanowires (red line) and simulation from a single crystal's structure (black line). (c) TEM image of **BPF** nanowires. (d) The SAED pattern of the single nanowire.

Figure 3. UV-vis absorption spectra of **BPF** in THF solution (a, black line) and **BPF** nanowires in aqueous solution (b, red line), Fluorescence spectra of **BPF** in THF (c, green line) and **BPF** nanowires in aqueous solution (d, blue line) with the excited wavelength at 356 nm.

Figure 4. EL spectra of **BPF** bulk or nanowire/*n*-SiC heterojunction LED biased at 30.5 V: (a) nanowire, (b) bulk state.

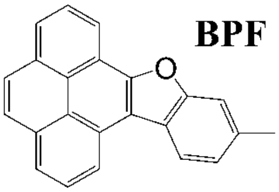

BPF

Scheme 1

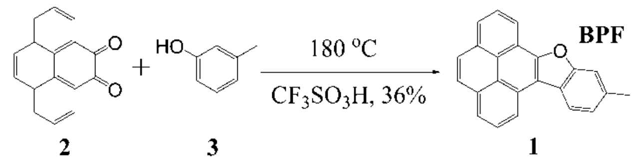

Scheme 2

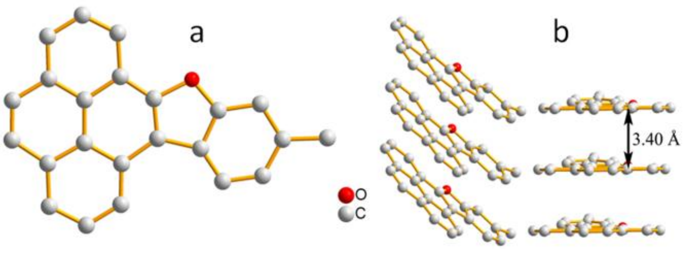

Figure 1

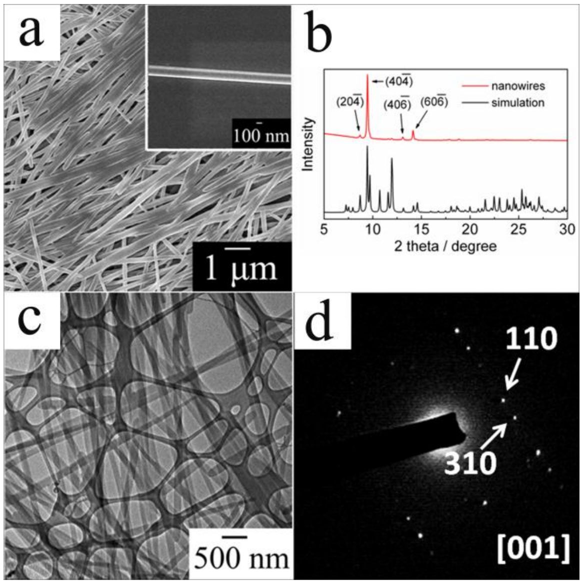
a
100 nm
1 μm
b
$(40\bar{4})$
$(20\bar{4})$
$(40\bar{6})$
$(60\bar{6})$
nanowires
simulation
Intensity
5
10
15
20
25
30
2 theta / degree
c
500 nm
d
110
310
[001]

Figure 2

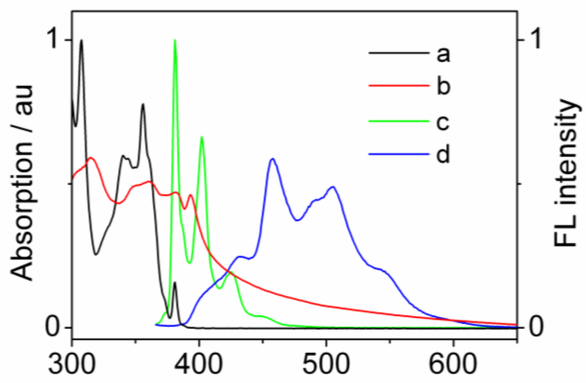

Figure 3

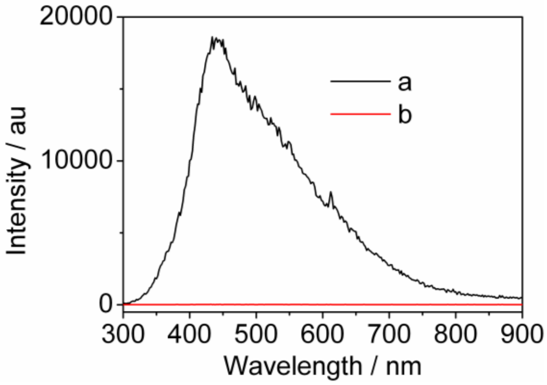
20000
10000
0
Intensity / au
300
400
500
600
700
800
900
Wavelength / nm
a
b

Figure 4